34th Annual International Conference of the IEEE EMBS
San Diego, California USA, 28 August - 1 September, 2012

Magnetic Resonance Based Noninvasive RF Nerve Stimulator

C V Ganesh Bharadwaj and Zheng Yuanjin

Abstract— **A noninvasive method of stimulating the nerve by applying radiofrequency has been presented. The design is based on the concept of magnetic resonance based power transfer. A comparison between electric field on the nerve at the frequency of 450-550 KHz with vacuum placed under a human tissue and the case where it is replaced with a resonant and non-resonant structure was analysed. Calculations were performed by using Ansoft HFSS. Power savings of 7.15% was observed when resonant structures were used, compared to vacuum. Theoretical calculation and simulation of fields were presented.**

I. Introduction

Recently there has been an increase in the research focussing on studying the effects due to time varying currents and magnetic fields in the frequency range of KHz-MHz [1]. Papers on transferring currents based on magnetic stimulation in the frequency range of 200 KHz-1 MHz has also been presented [2]. Neural stimulation at these high frequencies has been made possible through the use of ferrite cores using power amplifier topologies. The main concerns in magnetic stimulation include power requirement, and the electric field (E-field) at the nerve. Improving electrical fields by varying coil geometry were also proposed in literature, but these would need structural variation of equipment used for stimulation. Other methods not involving geometrical variations should be sort after.

Wireless power transfer using resonant structures was proposed for mid-range transfer [3]. However, this technology has not been effectively utilised in the biomedical industry for nerve stimulation. We initially present the concept of wireless power transfer using resonance mechanism and magnetic stimulation and how it can be combined at RF frequencies to be used to efficiently transfer current to the nerve.

A. Wireless Power Transfer using magnetic resonance

A system consisting of coupled resonances will operate in a strongly coupled region of operation and in this regime of operation, efficient energy transfer takes place.

Coupled mode theory helps in reducing the analysis of a physical system to a set of differential equations [3]. Assuming that one coil is driven, the following equations are obtained.

$$\dot{a}_S = -i(\omega_S - i\Gamma_S)a_S - ika_D + Fe^{-i\omega t} \quad (1)$$

$$\dot{a}_D = -i(\omega_D - i\Gamma_D)a_D - ika_S \quad (2)$$

Where ω_S and ω_D are the resonant frequencies of the isolated objects and Γ_S and Γ_D are the intrinsic decay rates due to absorption and radiated losses. k is the coupling co-efficient. F is the driving term and a is a variable defined so that the energy contained in the object is $|a_{S,D}(t)|^2$. When similar coils are used, the resonant frequency

$$f_0 = \frac{1}{2\pi\sqrt{LC}}. \quad (3)$$

Where

$$L = \frac{\mu_0}{4\pi|I_0|^2}\iint drdr'\frac{J(r).J(r')}{|r-r'|} \quad (4)$$

and

$$C = 4\pi\varepsilon_0|q_0|^2\frac{1}{\iint drdr'\frac{\rho(r).\rho(r')}{|r-r'|}} \quad (5)$$

J and ρ are the spatial current density and charge density respectively. If the receiver coil has a different resonant frequency than the source coil, then lower efficiency is observed. L and C are the effective inductance and capacitance of the resonating structures.

B. Magnetic Stimulation

Magnetic stimulation uses rate of change of current to change the magnetic field and hence causes a spatial rate of change of electric field along the length of the axon. The corresponding equation [4] is given by

$$\lambda_m{}^2\frac{\partial\overrightarrow{E_x}(x,t)}{\partial x} = \tau\frac{\partial V_m(x,t)}{\partial t} - \lambda_m{}^2\frac{\partial^2 V_m(x,t)}{\partial x^2} + V_m(x,t). \quad (6)$$

where

$$\lambda_m = \sqrt{\frac{r_m}{r_i}}\ and\ \tau_m = c_m r_m \quad (7)$$

Where the length and time constants are defined as λ_m and τ_m respectively, x is the distance along the axis of the nerve fiber when the nerve fiber is aligned along the x axis. E_x is the electric field along x axis. V_m is the trans-membrane voltage defined as the difference in voltage between the intracellular and extracellular fluid ($V_m = V_{intracellular} - V_{extracellular}$). r_m and r_i is the membrane resistance times unit length and the intracellular resistance respectively. c_m is the membrane capacitance per unit length. $\partial E_x/\partial x$ is the activation function.

*Research supported by National Medical Research council, Singapore.

CV Ganesh Bharadwaj is with the Nanyang Technological University, Singapore, (e-mail: ganesh5@e.ntu.edu.sg).

Zheng Yuanjin is with Nanyang Technological University, Singapore (e-mail: yjzheng@ntu.edu.sg).

This paper is divided into 4 sections. Section I is the introduction. Section II illustrates the chosen approach. Section III presents the simulation results and Section IV concludes the paper.

II. Approach

Let us examine the case of a coil which induces an electric field in the tissue below. The induced electric field can be calculated from the equation,

$$\vec{E}_{Source}(\vec{r}) = -\frac{\partial I_1}{\partial t}\frac{\mu_0}{4\pi}\int_S \frac{d\vec{l'}_{Source}}{|\vec{r}-\vec{r'}|} - \nabla\emptyset_1. \quad (8)$$

Where E is the electric field produced in the tissue due to a current carrying wire, $dl'$is an infinitesimal coil section and r' is the vector from each section to the point r. $\emptyset$ is the electric potential due to surface charge accumulation.

If a secondary coil, called the receiver coil is placed below the tissue, the vectorial addition of the fields due to the currents flowing through the source coil and the coil placed below the tissue result in increased electric field in the tissue. When maximum current flows through second coil due to resonance, the value of E is increased in some cases.

$$\vec{E}_{receiver}(\vec{r}) = -\frac{\partial I_2}{\partial t}\frac{\mu_0}{4\pi}\int_S \frac{d\vec{l'}_{receiver}}{|\vec{r}-\vec{r''}|} - \nabla\emptyset_2. \quad (9)$$

It should be noted that the resonant power transfer would result in only a percentage of current being transferred from the source to the receiver coil and hence while calculating the E-field due to the receiver coil, current is denoted as I_2, where $|I_2| < |I_1|$.

From the procedure detailed in [2, 5] we obtain the activation function $(\partial E_x/\partial x)$ shown in section I. B, mathematically after ignoring the secondary electric filed generated due to surface charge accumulation as shown in (10). x and y are the co-ordinates in the plane of the coil. s is the length of a side of the square coil. h is the total distance between the source and the receiver coil. p is the point at which the electric field is measured. x_0 and y_0 refer to points on the receiver coil. N denotes the number of turns in the primary coil and M refers to the number of turns in receiver coil. μ_{eq} is the effective permittivity detailed in [2].

For our analysis, electromagnetic simulators were employed to solve the field equations.

In this paper, the coil that is rotating in the anticlockwise direction when viewed from the source coil is called right hand and the coil that rotates in the clockwise direction when viewed from the source coil is called left hand coil.

III. Simulation and Results

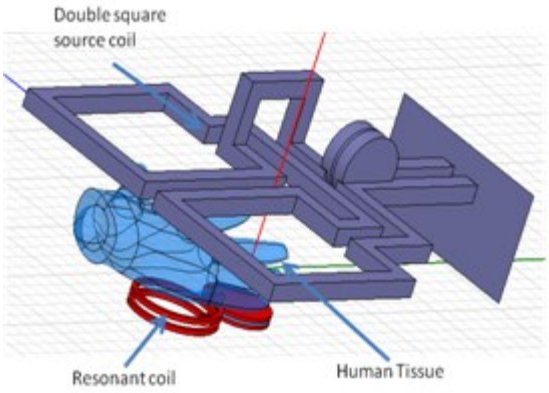

Fig. 1. Simulation set-up in Ansoft HFSS. Ferrite cores are avoided in figure to increase clarity

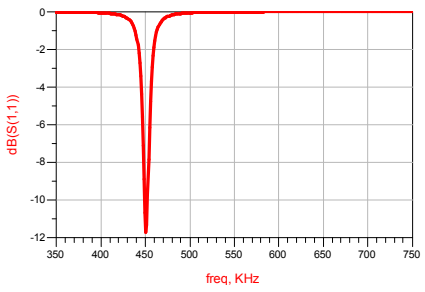

Fig. 2. Measurement of S11.

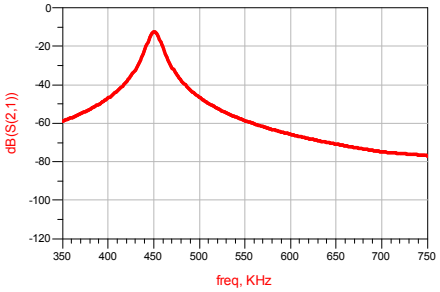

Fig. 3. Measurement of S21.

$$\frac{\partial E_x}{\partial x} = -\frac{\mu_{eq}}{4\pi}\left\{\left[N\left(\frac{dI_1}{dt}\right)\left(-\frac{2}{\sqrt{x^2+y^2+(h-p)^2}}+\frac{1}{\sqrt{(s-x)^2+y^2+(h-p)^2}}+\frac{1}{\sqrt{(s+x)^2+y^2+(h-p)^2}}-\frac{1}{\sqrt{(s-x)^2+(s-y)^2+(h-p)^2}}-\frac{1}{\sqrt{(s+x)^2+(s+y)^2+(h-p)^2}}+\frac{2}{\sqrt{x^2+(s-y)^2+(h-p)^2}}\right)\right] + \left[M\left(\frac{dI_2}{dt}\right)\left(\frac{1}{\sqrt{(x_0-x)^2+(y_0-y)^2+p^2}}\right)\right]\right\} \quad (10)$$

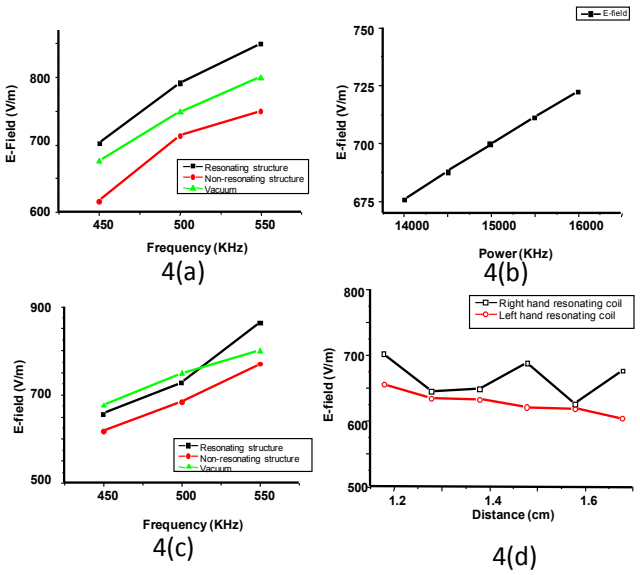

Fig. 4. (a) Right hand (anti-clockwise, while looking from top) resonating and non-resonating coils placed 1.179 cm below the source coil and vacuum measurement. (b) E-field plotted for varying input power. (c) Left hand (clockwise, while looking from top) resonating and non-resonating coils placed 1.179 cm below the source coil and vacuum measurement. (d) The variation in E-field with distance for left and right hand resonant coils at 450 KHz

Fig. 1 shows the simulation set up. Simulations were carried out in Ansoft HFSS. The simulation setup consists of the source coil, a tissue and a receiver coil below the tissue.

During simulations, to compare values, resonating structures and non-resonating structures were used as the receiver coil. Also in some cases, the coil was not used. Single windings were used for simplifying the source coil and wires were made as square prisms rather than cylindrical to avoid large computation time.

The double-square coil with ferrite cores was used as the source coil. Ferrite cores like the material 79 by Fair-rite co-operation can be used [6]. An input power of 14 KW was provided for the analysis. A part of the arm was used to represent the human body. Voxel models from the ITI'S foundation were used to extract tissue model parameters, that were used in the analysis [7]. These models are based on magnetic resonance images of people. Homogeneous models of fat were used in the simulation. Fields at 0.2 cm below the tissue was analysed. Simulations were performed with double-square coil placing non-resonant left and right hand coils, resonant left and right hand coils and vacuum under the tissue.

In our case the resonant coil placed below the tissue was satisfying the condition,

$$\sqrt{2L_rC_r} \leq R_r + R_L \tag{11}$$

Where L_r, C_r and R_r are the inductance, capacitance and resistance of the second coil and R_L is the load resistor. Equation (11) implies that the efficiency is larger at higher frequencies [8].

TABLE I. SOURCE AND RECIEVER COIL PARAMETERS

Frequency	$L_s(\mu H)$	$C_s(\mu F)$	$L_r(\mu H)$	$C_r(\mu F)$
450	0.203	0.615	0.136	0.92
500	0.203	0.498	0.136	0.745
550	0.203	0.412	0.136	0.616

And hence at high frequencies the efficiency of power transfer would increase considerably, than the results shown. This would result in more power savings for generating same E-field at the nerve.

The inductance and the capacitance chosen for the source and the receiver coil are shown in table 1. L_s and C_s represent inductance and capacitance of source coil. The inductance and capacitance shown in table I is calculated using (3), (4) and (5).

The source coil and the receiver coil has an intrinsic resistance given by R_s and R_r respectively. Because of skin effect, the current density on the surface of the wire is higher than that in the centre of the wire. When the resistance of the coils are calculated, this is to be accounted for. The resistance is given by [9].

$$R_r = \frac{2\pi aM}{\sigma 2\pi r\delta} \tag{12}$$

Where a is the radius of the coil (a=1.13cm), M is the number of turns (M=2), r is the cross sectional area of the wire (0.071 cm), σ is the conductivity of the wire. The material chosen for the wire is copper, which has a conductivity (σ=5.8·10^7). δ is the skin depth [9].

$$\delta = \frac{1}{\sqrt{\pi f \mu_0 \sigma}} \tag{13}$$

Where μ_0 is the permeability of free space (μ_0=4π·10^{-7}). Solving for δ and substituting in (12), we obtain R_r=5.58 mΩ at 450 KHz, 5.88 mΩ at 500 KHz and 6.17 mΩ at 550 KHz. The measurement in Fig. 2 and Fig. 3 is done by taking R_L as 50 Ω. R_r is negligible compared to R_L.

The source coil is a double-square coil with each side, s=5 cm. Number of turns, N=1. k is the number of coils. k is equal to 2, because the coil is a double-square coil. D is the width of the wire.

$$R_s = k \cdot \frac{4sN}{\sigma 4D\delta} \tag{14}$$

Which gives R_s=1.75 mΩ at 450 KHz, 1.845 mΩ at 500 KHz and 1.935 mΩ at 550 KHz.

High inductance and low capacitance value can be chosen for our purpose, but this would lead to increase in the size of the inductor, which makes the system impractical. Increasing the number of turns, can also increase the inductance and hence lead to increased efficiency. But this induces lot of simulation constraints and hence is not adopted in this paper. Our on-going work will also focus on experimentation, and we expect better results, due to the fact that, increased inductance can be easily introduced into the system.

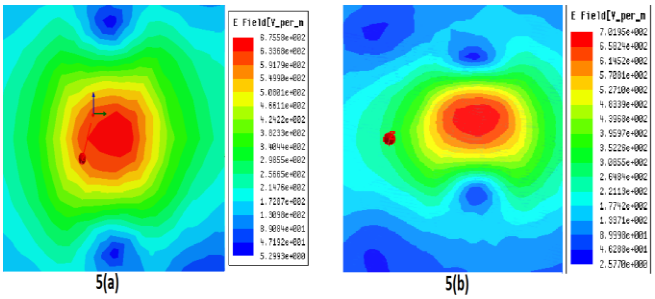

Fig. 5. (a) E-field when vacuum is placed under the tissue at 450 KHz. (b) E-field when right hand resonating coil is placed under tissue at 450 KHz. For a tissue thickness is 0.25 cm.

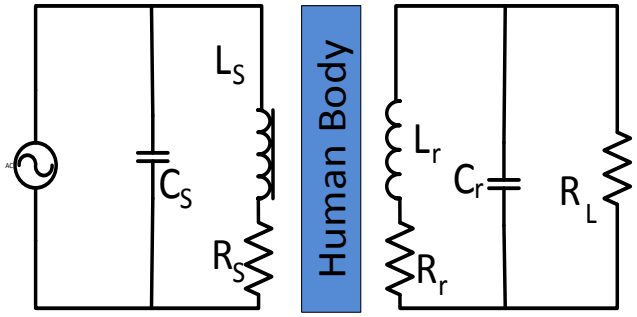

Fig. 6. Equivalent circuit diagram of proposed system

The initial work was to find out the frequency at which the coils resonate. For this purpose, a 2 port network was created in Ansoft HFSS.

Port 1 was the input to the double-square coil and the second port was chosen as the non-resonant structure with the same inductance as the resonating structure, but with negligible capacitance. These S-parameters were exported into Advanced Design System (ADS) and capacitors were added in parallel to the non-resonating system and the results were analysed.

The capacitor value was chosen so as to make the system resonate at 450 KHz, 500 KHz and 550 KHz respectively. The resonant frequency was chosen and at the frequency where maximum power transfer between the source coil and the receiver coil was observed. The S parameters for structures resonating at 450 KHz are shown in Fig. 2 and Fig. 3.

It can be seen from Fig. 4.a and Fig. 5 that for a right hand coil the E-field at a particular sheet in the tissue chosen is increased when a resonant coil is placed below it. At 450 KHz, for a tissue thickness of 0.25 cm, the electric field generated at 14 KW is 675.58 V/m. However, when power is increased the power reaches the value reached by the resonating structure at 701.95 V/m. Using vacuum below the tissue, a 7.15% increase in power would only lead to this increase in electric field as shown in Fig. 4.a which is illustrated with Fig. 4.b.

Fig. 6 shows the equivalent circuit model for the system. It should be noted that the non-resonant coil used in the simulations had the same inductance, but very low capacitance, leading it to resonate at much higher frequencies. This work helps in reducing power for analysis equipment used at these high frequencies. Improved electric fields were observed when resonant structures are used instead of vacuum even at reduced input power supply.

But with varying distance from the source coil, the E-field also varies. The variation in E-field with distance for left and right hand resonant coils were plotted in Fig. 4.d. If the tissue thickness increases, the increase in E-field becomes less substantial. For experimental calculation of E-field and analysis of tissue parameters, this paper can prove to be a pedestal.

IV. Conclusion

In this paper, for the first time, the principle of magnetic resonance has been used to simulate the generation of increased fields in the order of KHz for stimulation in the nerve between the tissues. The results indicated 7.15% power savings for generating the same E-field at 450 KHz. The paper also illustrates that resonant structures and coils can be used as a tool for varying the E-field in a particular region of a tissue. Other coils like figure-of-eight coils can also be used together with resonating structures. If higher power transfer efficiencies are observed this would result in higher electric fields at the nerve for lower power consumption.

This paper provides a theoretical basis and EM analysis for a non-invasive RF stimulator based on magnetic resonance. Work with heterogeneous simulation models and experiment with real tissue will help validate the work presented in this paper. Experiment will be carried out in future work to estimate the feasibility of the concept.

Acknowledgment

Ganesh Bharadwaj CV thanks Economic Development Board, Singapore for providing him the ICPS scholarship.

References

[1] J. Bohnert, *et al.*, "Effects of time varying currents and magnetic fields in the frequency range of 1 kHz to 1 MHz to the human body - a simulation study," in *Engineering in Medicine and Biology Society (EMBC), 2010 Annual International Conference of the IEEE*, 2010, pp. 6805-6808.

[2] E. Basham, *et al.*, "Circuit and Coil Design for In-Vitro Magnetic Neural Stimulation Systems," *IEEE Transactions on Biomedical Circuits and Systems,* vol. 3, pp. 321-331, 2009.

[3] A. Karalis, *et al.*, "Efficient wireless non-radiative mid-range energy transfer," *Annals of Physics,* vol. 323, pp. 34-48, 2008.

[4] B. J. Roth and P. J. Basser, "A model of the stimulation of a nerve fiber by electromagnetic induction," *IEEE Transactions on Biomedical Engineering,* vol. 37, pp. 588-597, 1990.

[5] K. P. Esselle and M. A. Stuchly, "Neural stimulation with magnetic fields: analysis of induced electric fields," *IEEE Transactions on Biomedical Engineering,* vol. 39, pp. 693-700, 1992.

[6] *http://www.fair-rite.com/*.

[7] A. Christ, *et al.*, "The Virtual Family—development of surface-based anatomical models of two adults and two children for dosimetric simulations " *Physics in Medicine and Biology,* vol. 55, pp. 23-38, 2010.

[8] L. Peng, *et al.*, "wireless energy transfer through non-resonant magnetic coupling," *J. of Electromagnetic waves and applications,* vol. 24, pp. 1587-1598, 2010.

[9] B. L. Cannon, *et al.*, "Magnetic Resonant Coupling As a Potential Means for Wireless Power Transfer to Multiple Small Receivers," *IEEE Transactions on Power Electronics,* vol. 24, pp. 1819-1825, 2009.